Low-Complexity Acoustic Scene Classification Using Data Augmentation and Lightweight ResNet

Yanxiong Li
School of Electronic and Information Engineering, South China University of Technology, Guangzhou, China
eeyxli@scut.edu.cn

Wenchang Cao
School of Electronic and Information Engineering, South China University of Technology, Guangzhou, China
wenchangcao98@163.com

Wei Xie
School of Electronic and Information Engineering, South China University of Technology, Guangzhou, China
chester.w.xie@gmail.com

Qisheng Huang
School of Electronic and Information Engineering, South China University of Technology, Guangzhou, China
839508665@qq.com

Wenfeng Pang
School of Electronic and Information Engineering, South China University of Technology, Guangzhou, China
wenfengpang@gmail.com

Qianhua He
School of Electronic and Information Engineering, South China University of Technology, Guangzhou, China
eeqhhe@scut.edu.cn

***Abstract*—We present a work on low-complexity acoustic scene classification (ASC) with multiple devices, namely the subtask A of Task 1 of the DCASE2021 challenge. This subtask focuses on classifying audio recordings of multiple devices with a low-complexity model, where two main difficulties need to be overcome. First, the audio recordings are recorded by different devices, and there is mismatch of recording devices in audio recordings. We reduce the negative impact of the mismatch of recording devices by using some effective strategies, including data augmentation (e.g., mix-up, spectrum correction, pitch shift), usages of multi-patch network structure and channel attention. Second, the model size should be smaller than a threshold (e.g., 128 KB required by the DCASE2021 challenge). To meet this condition, we adopt a ResNet with depthwise separable convolution and channel attention as backbone network, and perform model compression. In summary, we propose a low-complexity ASC method using data augmentation and a lightweight ResNet. Evaluated on the official development and evaluation datasets, our method obtains classification accuracy scores of 71.6% and 66.7%, respectively; and obtains Log-loss scores of 1.038 and 1.136, respectively. Our final model size is 110.3 KB which is lower than the limit of 128 KB.**

Keywords—acoustic scene classification, lightweight ResNet, data augmentation, depthwise separable convolution, channel attention

I. INTRODUCTION

Acoustic scene classification (ASC) is a task to classify each audio recording into one class of pre-given acoustic scenes. As an important task in the challenge on Detection and Classification of Acoustic Scenes and Events (DCASE) [1], ASC has attracted many attentions from researchers in the community of audio and acoustic signal processing in recent years [2]-[26]. With the development of the study on the ASC problem, some state-of-the-art techniques are proposed to solve the ASC problem.

In this work, we focus on the task of low-complexity ASC with multiple devices which is the subtask A of Task 1 of the DCASE2021 challenge [27]. This task requires to classify audio recordings recorded by multiple devices (real and simulated) through a low-complexity model. To deal with the mismatch of recording devices in audio recordings, many researchers have proposed many methods which are mainly divided into two types: data processing and model building.

The first type concentrates on front-end data processing. Audio recordings acquired by various devices generally have different time-frequency properties. One common practice for alleviating the negative impact of recording device mismatch is to collect as many audio recordings as possible from different recording devices, but it requires a lot of manpower. In addition, more audio recordings can be also obtained by some low-cost and effective ways, such as spectrum correction, frequency shift, mix-up [28], [29].

The second type focuses on back-end model building, where the model is designed to have the abilities to distinguish different types of acoustic scenes and to avoid the influence of different devices. The methods based on the models of convolutional neural network (CNN) and the CNN's variants are dominant solutions for ASC tasks [4]-[9], [30]-[36]. The CNN has powerful ability to learn discriminative information from its input spectrogram which is one of the most effective and widely used audio features in ASC task. In addition, some researchers modify existing networks and apply them to the ASC task with satisfactory results. For example, McDonnell et al separate the ResNet into two pathways, and the separation of high and low frequencies is proved to be effective for enhancing the network's adaptability to multi-device audio recordings [33]. Koutini et al explore the influence of receptive field on the performance of ASC methods [34]. Su et al modify the Xception network to build their model for making prediction [35].

The works above have promoted the development of ASC, but there are still shortcomings when they are used to tackle the problem of low-complexity ASC. For example, the model size in these methods is very large, and these methods are not robust to multiple devices. Inspired by the successes of data augmentation and CNN-based models for audio and vision classification in previous works, we propose a method for low-complexity ASC using data augmentation techniques and a lightweight ResNet with channel attention (CA). In our method, depthwise separable convolution (DSC) [37] instead of standard convolution is used as the basic module for building a lightweight ResNet, and the CA is adopted to utilize channel information after DSC. In addition, some data augmentation techniques are adopted to mitigate the negative influence of recording devices mismatch on our method. Experimental results have proved the effectiveness of the proposed method. In short, the contributions of this work are as follows:

1) We propose a low-complexity ASC method using data

Corresponding author: Yanxiong Li (eeyxli@scut.edu.cn).

This work was supported by national natural science foundation of China (62111530145, 61771200), international scientific research collaboration project of Guangdong Province (2021A0505030003), and Guangdong basic and applied basic research foundation (2021A1515011454).

augmentation techniques and a lightweight network with CA.

2) We discuss contributions of main modules of our method (e.g., CA, data augmentation), and compare our method with baseline method on public and official datasets.

II. METHOD

As shown in Fig. 1, the framework of our method includes two parts: data augmentation and model building.

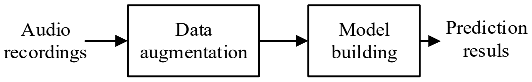

Fig. 1: *The framework of our method.*

A. Data Augmentation

To reduce the negative impact of the recording device mismatch on the performance of our method, some data augmentation techniques are adopted in our method. These techniques are described as follows.

The first technique is mix-up which is theoretically simple but effective [29]. It makes our model behave consistently to training samples from different devices. This modeling technique can enhance robustness of the model on training samples. The mix-up algorithm adopted in our paper is theoretically consistent with the original one. In practical implementation, our practice for mix-up is slightly different from original one in [29]. In each time, we load two batches of audio recordings instead of two audio recordings (used by [29]), into memory and process them by $X' = \lambda X_i + (1\text{-}\lambda)X_j$. X_i and X_j are two batches of audio recordings from the shuffled training data, and λ obeys Beta distribution, i.e. $\lambda \sim \text{Beta}(\alpha, \alpha)$ and α is experimentally set to 0.4. Through loading two batches of audio recordings, more information can be used during the procedure of mixing, which is beneficial for improving the performance of our method.

The second technique is spectrum correction which shows moderate device adaptation properties [38]. However, in this work, it is adjusted before it is applied for ASC. The spectrum correction in this work aims at transforming the given input spectrum into a corrected spectrum using an ideal device (a reference device). The implementation of spectrum correction consists of two steps. First, we need a correction coefficient which can be obtained by calculating the average of n pairs of aligned spectra. Here, the value of n is experimentally set to 150. The correction coefficient of device A to the reference device is the ratio of the frequency response of the reference device to the frequency response of device A. The frequency response of the reference device is the average of the frequency responses of multiple devices. In the second step, the corrected spectrum of device A can be obtained by multiplying the correction coefficient with the original spectrum of the audio recordings recorded by device A.

The third technique is pitch shift [39], which is to resample the original audio recordings at various sampling frequencies with a certain step size. The pitches of audio recordings recorded by various devices are generally different to each other, which is helpful for ASC. Hence, pitch shifting is performed before extracting log-Mel spectrogram (LMS) from each audio recording.

The fourth technique is audio-mix which is inspired by the work in [40]. We randomly mix two audio recordings from the same acoustic scene for simulating more devices, smoothing transition among devices, and reducing differences among different devices.

B. Model Building

Our model is a lightweight ResNet which inherits merits from MobileNet [41] and ResNet [42], whose main module is inverted residual blocks with DSC and CA. The motivation for the adoption of DSC and CA is based on two reasons. Firstly, the DSC can remarkably decrease the model's size. Second, the CA can make the model focus on the critical channel information which is not efficiently used during the operation of DSC. As a result, the integration of the DSC and CA into the inverted residual blocks is expected to be able to make our model more concise with better generalization performance for ASC with multiple devices, which is also one technical contribution of this work.

Framework of Our Model

As shown in Fig. 2, our model is a deep architecture consisting of two pathways of inverted residual blocks with DSC and CA, maximum and global average pooling layers, fully-connected and Softmax layers. The motivation for the usage of two pathways of inverted residual blocks is that deep feature maps learned by two pathways of inverted residual blocks are expected to be more effective for representing the differences of time-frequency properties among various acoustic scenes and thus obtain a better result compared to one pathway of inverted residual blocks.

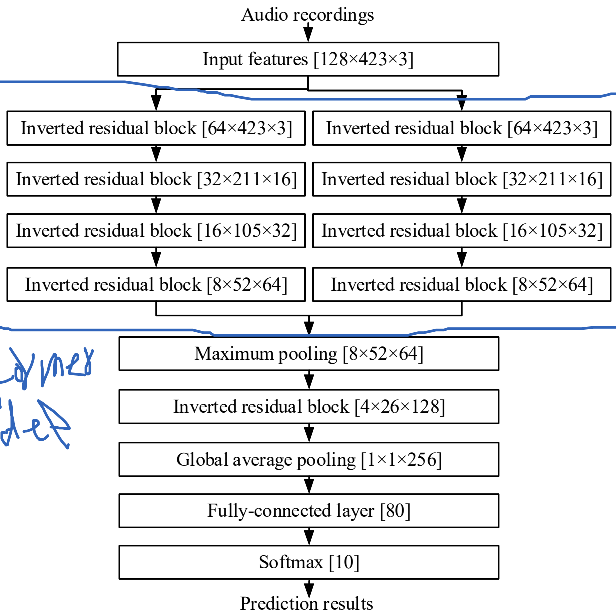

Conformer Model

Fig. 2: *Framework of our model.*

Our model's structure and parameters are shown in Fig. 2. The three digits in the square bracket, such as 32, 211 and 16 in [32×211×16], represent height of the input feature map, width of the input feature map, and number of channels, respectively. Our model works as follows. First, input features are extracted from audio recordings and then are split into two subsets along the first dimension (the dimension of filter-bank) of input features. Next, the two subsets of input features are fed to two pathways of inverted residual blocks in parallel. Afterwards, the outputs of these two pathways of inverted residual blocks are concatenated along the first dimension of input features and then their concatenation is sequentially fed to one maximum pooling layer, one inverted residual block and one global average pooling layer for further transformation. Finally, the transformed feature map is flattened by a fully-connected layer and then fed to a Softmax layer to make a prediction of acoustic scene for each input audio recording.

Inverted Residual Block

The inverted residual block with DSC and CA is the novel part of our model. One convolutional kernel of the DSC is responsible for one channel, and one channel is convoluted by only one convolutional kernel. The DSC is implemented by decomposing the standard convolution into two steps: depthwise convolution and 1×1 pointwise convolution [37]. Depthwise convolution applies a single filter to each input channel, and pointwise convolution uses 1×1 convolution to combine the outputs of different depthwise convolutions. The framework of one inverted residual block is depicted in Fig. 3, which mainly includes the layers of DSC, batch normalization, ReLU, channel attention, and Maximum pooling.

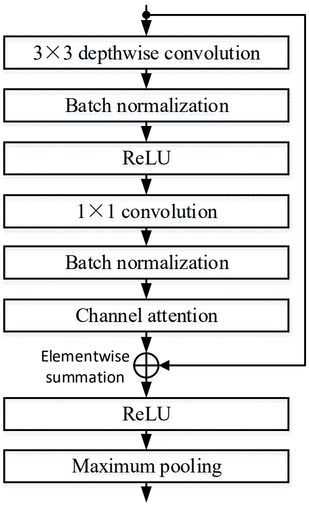

Fig. 3: *Framework of one inverted residual block.*

Channel Attention

A channel attention mechanism [43] is introduced to our model, whose framework is shown in Fig. 4. The dimension of input feature $\boldsymbol{F}$ is $H\times W\times C$, where H, W and C denote height of the input feature map, width of the input feature map, and number of channels, respectively. First, average pooling (AvgPool) and maximum pooling (MaxPool) are performed on the input feature $\boldsymbol{F}$ for obtaining two channel descriptions with dimension of $1\times1\times C$. Then, these two channel descriptions are independently fed to a multi-layer perceptron (MLP) for obtaining their respective transformed features. That is, this MLP is shared for these two channel descriptions. Afterwards, the weight coefficient $\boldsymbol{M}_C$ is obtained by element-wisely summing these two transformed features from the MLP followed by a Sigmoid activation function. Finally, a new scaled feature $\boldsymbol{F'}$ is obtained by multiplying the weight coefficient $\boldsymbol{M}_C$ with the input feature $\boldsymbol{F}$.

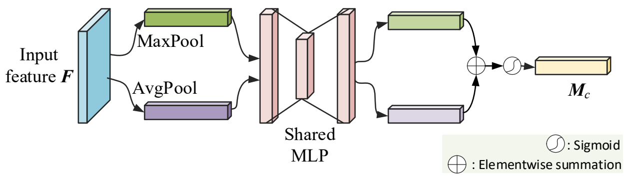

Fig. 4: *Framework of channel attention*.

III. Experiments

In this section, we will present experimental data, setup, results, and discussions in detail.

A. Experimental Data

Experimental data consists of development dataset and evaluation dataset and has 10 types of acoustic scenes, which is publicly available for research purpose on the website of the DCASE2021 challenge [44]. The development dataset consists of training subset and validation subset. The training and validation subsets have 13962 and 2968 audio recordings, respectively. The development dataset contains audio recordings from 10 cities and 9 devices: 3 real devices (A, B, C) and 6 simulated devices ($S1$-$S6$). Audio recordings of devices B, C, and $S1$-$S6$ are randomly selected from the audio segments of simultaneous recordings. Audio recordings of devices B, C, and $S1$-$S6$ overlap with the audio recordings of device A, but not overlap with each other. The total amount of audio recordings in the development dataset is 64 hours. In the development dataset, the data proportions of training subset and validation subset are 70% and 30%, respectively. The evaluation dataset contains audio recordings from 12 cities, 11 devices. There are six new devices (not in the development dataset): a real device D and simulated devices $S7$-$S11$. The evaluation dataset contains 22 hours of audio recordings.

B. Experimental Setup

All audio recordings are saved as: 44.1 kHz sampling rate, 16 bits quantization, and mono channel. Audio recordings are first divided into frames via a hamming window whose length is 2048 with 50% overlapping. Short-time Fourier transform is then performed on each frame for obtaining linear power spectrum which is finally smoothed with a bank of triangular filters for producing LMS. The center frequencies of these triangular filters are uniformly spaced on the Mel-scale. In addition, to enhance the discriminative ability of audio feature, the delta, and delta-delta coefficients of the LMS are calculated, and then they are stacked along channel axis and used as input feature. The input feature size is: 128×423×3, where 128, 423 and 3 are the numbers of filter-bank, frame and channel, respectively. The three channels are the LMS, the delta coefficients of the LMS, and the delta-delta coefficients of the LMS.

The baseline method is a combination of a CNN and a feature of log Mel-band energies. The CNN used in the baseline method consists of three convolutional layers and one fully-connected layer. The details of the baseline method are referred to [44]. The major difference between our method and the baseline method is the back-end model. That is, our model mainly consists of two pathways of inverted residual blocks with DSC and CA, whereas the model in the baseline method is a common CNN with standard convolution without DSC and CA.

All experiments are done using the toolkit of Keras. Adam is used as the optimizer, and categorical cross entropy is adopted as the loss function. Classification accuracy (the higher the better) and log-loss (the lower the better) are used as performance metrics. Adam's initial value is set to 0.001, and cosine annealing algorithm is used as the learning strategy. There is a cosine relationship between training epochs and learning rate. The maximum and minimum learning rates are set to 10^{-3} and 10^{-7}, respectively. The batch size is set to 16. The checkpoint with the highest validation accuracy is used as the best model. The models are trained using 3 different seeds and choose the average accuracy as final result.

In subtask A of Task 1 of DCASE2021 challenge, the limit of space-complexity for the model is 128 KB excluding zero parameters. That is, the model contains at most 32768 parameters when each parameter is represented by 32-bit floating numbers (i.e., 32768 parameters × 32 bits/parameter = 128 × 8 bits/Byte × 1024 Bytes = 128 KB). To meet this requirement, besides the adoption of lightweight ResNet with DSC and CA, a quantization operation is performed for further compressing our trained model. The quantization method is provided by Tensorflow2 [43] which is adopted to convert the 32-bit floating parameters of our model into the 16-bit floating parameters. Specifically, floating-point numbers are saved by scientific counting method. During the process of converting 32-bit to 16-bit floating numbers, the sign and exponential bits remain unchanged, and the first half part of the numeric bits of each 32-bit floating number are used as numeric bits of the 16-bit floating number.

C. Experimental Results

Table I lists the contribution of CA to our and baseline methods in terms of classification accuracy on the development dataset without data augmentation. Classification accuracies of two methods are upgraded after adopting CA. For example, our method with CA obtains classification accuracy improvement by 1.8% (67.2% - 65.4%), compared to our method without CA.

TABLE I. CLASSIFICATION ACCURACIES OBTAINED BY OUR METHOD AND BASELINE METHOD WITH OR WITHOUT CA

	Baseline	Ours
without channel attention	49.8%	65.4%
with channel attention	51.3%	67.2%

Table II shows the contributions of various data augmentation techniques to the increase of classification accuracies for our and baseline methods on the development dataset. Classification accuracies of these two methods are increased after introducing data augmentation techniques, and every data augmentation technique contributes to performance improvement of these two methods. Moreover, our and baseline methods obtain the highest classification accuracies of 71.4% and 54.9%, respectively, when all data augmentation techniques are adopted. For example, our method with mix-up and spectrum correction techniques obtains classification accuracy improvement by 1.9% (69.1% - 67.2%) and 2.4% (69.6% - 67.2%), respectively, compared with the methods without any data augmentation techniques. Among these data augmentation techniques, pitch shift technique produces the highest improvement by 3.3% (70.5% - 67.2%) for our method, while the technique of mix audio generates the highest improvement by 3.2% (54.5% - 51.3%) for the baseline method. The reasons why pitch shift and mix audio are more effective than other techniques are that larger noise interferences are integrated into the original audio recordings, and these noise interferences enlarge the differences of time-frequency characteristics among the audio recordings of different recording devices. Hence, they can produce higher performance gain.

TABLE II. CLASSIFICATION ACCURACIES OBTAINED BY OUR METHOD AND BASELINE METHOD WITH OR WITHOUT DATA AUGMENTATION TECHNIQUES

Data augmentation techniques	Baseline	Ours
None (without any techniques)	51.3%	67.2%
Mix-up	52.4%	69.1%
Spectrum correction	53.1%	69.6%
Pitch shift	54.2%	70.5%
Mix audio	54.5%	69.9%
All above	54.9%	71.4%

Table III shows the results of both baseline method and our method on the development dataset. The number of non-zero parameters and model size of our method are larger than the counterparts of baseline method, and the margins of the number of non-zero parameters and model size between the baseline method and our method are 8800 (56486 - 47686) and 20 KB (110.3 -90.3 KB), respectively. Our method is heavier than the baseline method in terms of both the number of non-zero parameters and model size. Our method outperforms the baseline method in terms of classification accuracy. The margin of classification accuracy between the baseline and our methods is 16.5%. In addition, our model size after quantization compression is 110.3 KB (56486 parameters × 16 bits/parameter = 110.3 × 8 bits/Byte × 1024 Bytes = 110.3 KB) which is smaller than the size limit of 128 KB.

TABLE III. RESULTS OF BASELINE AND OUR METHODS

Model	Accuracy	Number of non-zero parameters	Model size(KB)
Baseline	54.9%	47686	90.3
Ours	71.4%	56486	110.3

To know the confusions among different acoustic scenes, Fig. 5 shows the confusion matrix obtained by our method on the development dataset. The accuracies for *Airport*, *Public square*, and *Street pedestrian* are lower than that for other acoustic scenes. The reason is that these three acoustic scenes have larger intra-class differences. In addition, the confusions between *Airport* and *Shopping mall* are larger than that between other pairs of acoustic scenes. The reason is that the time-frequency properties of these two acoustic scenes are more similar. As a result, they are more easily confused with each other.

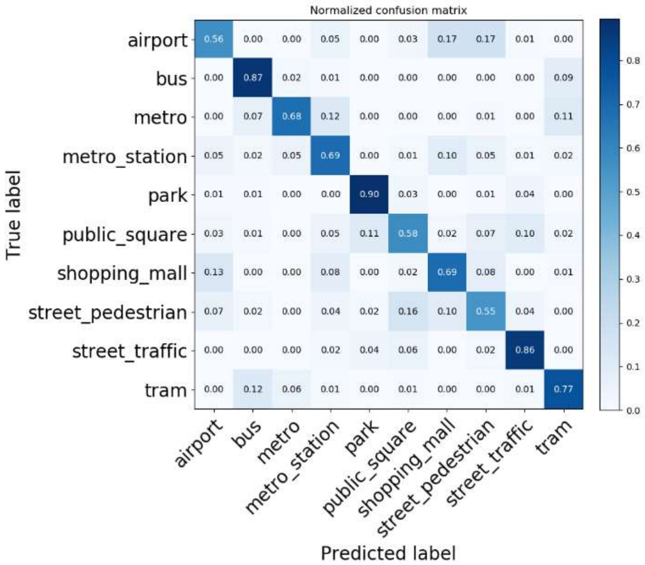

Fig. 5: *Confusion matrix of our method on the development dataset*.

Finally, we evaluate our method on the evaluation dataset. It should be noted that the labels of the evaluation dataset are not publicly available and the results in Table IV are given by the organizer of the DCASE2021 challenge [44]. As shown in Table IV, our method obtains Log-loss score of 1.136 and classification accuracy score of 66.7%, and outperforms the baseline method in terms of both Log-loss and classification accuracy.

TABLE IV. RESULTS OBTAINED BY OUR METHOD AND BASELINE METHOD ON THE EVALUATION DATASET

Acoustic scenes	Baseline		Ours	
	CA (%)	Log-loss	CA (%)	Log-loss
Airport	24.0	2.077	43.7	1.461
Bus	44.6	1.615	77.0	1.007
Metro	54.4	1.159	67.2	1.169
Metro station	37.8	1.955	59.3	1.343
Park	52.7	2.173	84.1	0.753
Public square	24.4	2.455	49.9	1.485
Shopping mall	63.8	1.227	77.3	1.006
Street pedestrian	39.9	1.744	41.9	1.576
Street traffic	56.4	1.825	85.0	0.618
Tram	58.1	1.073	81.6	0.937
Average	45.6	1.730	66.7	1.136

IV. CONCLUSIONS

We presented our work on the low-complexity ASC with multiple devices. We proposed a method by a lightweight ResNet with DSC and CA. The whole network's structure and some strategies designed in this paper are novel. For example, the DSC is adopted to make our network light enough, and the CA is integrated into the inverted residual block to exchange channel information. In addition, considering the differences of time-frequency properties among different frequency bands of audio feature, we first divide the input audio feature into two parts: low-frequency and high-frequency parts along the dimension of frequency axis, and then fuse them.

Our method exceeded baseline method in terms of Log-loss and classification accuracy. Moreover, the size of our model is

110.3KB, and is lower than the size limit of 128 KB. Our method is effective for solving the low-complexity ASC problem. Limitations of our method are that front-end data augmentation and back-end model building are separately instead of jointly implemented, and that only one model instead of multi-model combination is adopted. The next works include exploring other model structures, designing the techniques of data augmentation, jointly optimizing both front-end data augmentation and back-end model building, and assembling models.

REFERENCES

[1] T. Heittola, A. Mesaros, and T. Virtanen, “Acoustic scene classification in DCASE 2020 challenge: generalization across devices and low complexity solutions,” in *Proc. of DCASE Workshop*, 2020.

[2] Y. Li, X. Li, Y. Zhang, W. Wang, M. Liu, and X. Feng, “Acoustic scene classification using deep audio feature and BLSTM network,” in *Proc. of ICALIP*, 2018, pp. 371-374.

[3] S. Singh, H. L. Bear, and E. Benetos, “Prototypical networks for domain adaptation in acoustic scene classification,” in *Proc. of IEEE ICASSP*, 2021, pp. 346-350.

[4] Y. Liu, A. Neophytou, S. Sengupta, and E. Sommerlade, “Cross-modal spectrum transformation network for acoustic scene classification,” in *Proc. of IEEE ICASSP*, 2021, pp. 830-834.

[5] H. Hu et al., “A two-stage approach to device-robust acoustic scene classification,” in *Proc. of IEEE ICASSP*, 2021, pp. 845-849.

[6] Y. Li, M. Liu, W. Wang, Y. Zhang and Q. He, “Acoustic scene clustering using joint optimization of deep embedding learning and clustering iteration,” *IEEE TMM*, vol. 22, no. 6, pp. 1385-1394, 2020.

[7] Z. Ren, Q. Kong, J. Han, M. D. Plumbley, and B. W. Schuller, “CAA-Net: conditional atrous CNNs with attention for explainable device-robust acoustic scene classification,” *IEEE TMM*, 2020.

[8] S. S. R. Phaye, E. Benetos, and Y. Wang, “SubSpectralNet - using sub-spectrogram based convolutional neural networks for acoustic scene classification,” in *Proc. of IEEE ICASSP*, 2019, pp. 825-829.

[9] S. Takeyama, T. Komatsu, K. Miyazaki, M. Togami, and S. Ono, “Robust acoustic scene classification to multiple devices using maximum classifier discrepancy and knowledge distillation,” in *Proc. of EUSIPCO*, 2021, pp. 36-40.

[10] A. I. Mezza, E. A. P. Habets, M. Müller, and A. Sarti, “Unsupervised domain adaptation for acoustic scene classification using band-wise statistics matching,” in *Proc. of EUSIPCO*, 2021, pp. 11-15.

[11] V. Abrol, and P. Sharma, “Learning hierarchy aware embedding from raw audio for acoustic scene classification,” *IEEE/ACM TASLP*, vol. 28, pp. 1964-1973, 2020.

[12] M. C. Green, S. Adavanne, D. Murphy, and T. Virtanen, “Acoustic scene classification using higher-order ambisonic features,” in *Proc. of IEEE WASPAA*, 2019, pp. 328-332.

[13] L. Pham, I. McLoughlin, H. Phan, R. Palaniappan, and A. Mertins, “Deep feature embedding and hierarchical classification for audio scene classification,” in *Proc. of IJCNN*, 2020, pp. 1-7.

[14] Y. Wu, and T. Lee, “Time-frequency feature decomposition based on sound duration for acoustic scene classification,” in *Proc. of IEEE ICASSP*, 2020, pp. 716-720.

[15] K. Drossos, P. Magron, and T. Virtanen, “Unsupervised adversarial domain adaptation based on the Wasserstein distance for acoustic scene classification,” in *Proc. of IEEE WASPAA*, 2019, pp. 259-263.

[16] C. Paseddula, and S. V. Gangashetty, “Acoustic scene classification using single frequency filtering cepstral coefficients and DNN,” in *Proc. of IEEE IJCNN*, 2020, pp. 1-6.

[17] X. Bai, J. Du, J. Pan, H.S. Zhou, Y.H. Tu, and C.H. Lee, “High-resolution attention network with acoustic segment model for acoustic scene classification,” in *Proc. of IEEE ICASSP*, 2020, pp. 656-660.

[18] S. Mun, and S. Shon, “Domain mismatch robust acoustic scene classification using channel information conversion,” in *Proc. of IEEE ICASSP*, 2019, pp. 845-849.

[19] W. Xie, Q. He, Z. Yu, and Y. Li, “Deep mutual attention network for acoustic scene classification,” *Digital Signal Processing*, vol.123, 2022.

[20] L. Pham, H. Phan, T. Nguyen, R. Palaniappan, A. Mertins, and I. McLoughlin, “Robust acoustic scene classification using a multi-spectrogram encoder-decoder framework,” *Digital Signal Processing*, vol. 110, 2021.

[21] J.-w. Jung, H.-j. Shim, J.-h. Kim, and H.-J. Yu, "DCASENET: An integrated pretrained deep neural network for detecting and classifying acoustic scenes and events," in *Proc. of IEEE ICASSP*, 2021, pp. 621-625.

[22] C. Paseddula, and S.V. Gangashetty, “Late fusion framework for acoustic scene classification using LPCC, SCMC, and log-Mel band energies with deep neural networks,” *Applied Acoustics*, vol. 172, 2021.

[23] M.A. Alamir, “A novel acoustic scene classification model using the late fusion of convolutional neural networks and different ensemble classifiers,” *Applied Acoustics*, vol. 175, 2021.

[24] K. Imoto, “Acoustic scene classification using multichannel observation with partially missing channels,” in *Proc. of EUSIPCO*, 2021, pp. 875-879.

[25] S. Song, B. Desplanques, C. De Moor, K. Demuynck, and N. Madhu, “Robust acoustic scene classification in the presence of active foreground speech,” in *Proc. of EUSIPCO*, 2021, pp. 995-999.

[26] J. Zhao, Q. Kong, X. Song, Z. Feng, and X. Wu, “Feature alignment for robust acoustic scene classification across devices,” in *IEEE Signal Processing Letters*, 2022, doi: 10.1109/LSP.2022.3145336.

[27] I. Martín-Morató, T. Heittola, A. Mesaros, and T. Virtanen, “Low-complexity acoustic scene classification for multi-device audio: analysis of DCASE 2021 challenge systems,” 2021.arXiv:2105.13734.

[28] M. Kośmider, “Calibrating neural networks for secondary recording devices,” in *Tech. Rep of DCASE2019 Challenge*.

[29] H. Zhang, M. Cisse, Y. N. Dauphin, and D. LopezPaz, “MixUp: Beyond empirical risk minimization,” in *Proc. of ICLR*, 2018, pp.1-13.

[30] D. Barchiesi, D. Giannoulis, D. Stowell, and M. D. Plumbley, “Acoustic scene classification: Classifying environments from the sounds they produce,” *IEEE SPM*, vol. 32, no. 3, pp. 16-34, 2015.

[31] H.K. Chon, Y. Li, W. Cao, Q. Huang, W. Xie, W. Pang, and J. Wang, “Acoustic scene classification using aggregation of two-scale deep embeddings,” in *Proc. of IEEE ICCT*, 2021, vol. 4, pp. 1341-1345.

[32] J. Salamon and J.P. Bello, “Deep convolutional neural networks and data augmentation for environmental sound classification,” *IEEE SPL*, vol. 24, no. 3, pp. 279-283, 2017.

[33] M.D. McDonnell and W. Gao, “Acoustic scene classification using deep residual networks with late fusion of separated high and low frequency paths,” in *Proc. of IEEE ICASSP*, 2020, pp. 141-145.

[34] K. Koutini, H. Eghbal-zadeh, G. Widmer, and J. Kepler, “CP-JKU submissions to DCASE’19: Acoustic scene classification and audio tagging with receptive-field-regularized CNNs,” in *DCASE Challenge*, 2019, pp. 1-5.

[35] Y. Su, K. Zhang, J. Wang, and K. Madani, “Environment sound classification using a two-stream CNN based on decision-level fusion,” *Sensors*, vol. 19, no. 7, pp. 1-15, 2019.

[36] Y. Zeng, Y. Li, Z. Zhou, R. Wang, and D. Lu, “Domestic activities classification from audio recordings using multi-scale dilated depthwise separable convolutional network,” in *Proc. of IEEE MMSP*, Tampere, Finland, 2021, pp. 1-5.

[37] K. Drossos, S.I. Mimilakis, S. Gharib, Y. Li, and T. Virtanen, “Sound event detection with depthwise separable and dilated convolutions,” in *Proc. of IJCNN*, 2020, pp. 1-7.

[38] T. Nguyen, F. Pernkopf, and M. Kosmider, “Acoustic scene classification for mismatched recording devices using heatedup Softmax and spectrum correction,” in *Proc. of IEEE ICASSP*, 2020, pp. 126-130.

[39] S. Watanabe, and M. Tsuzaki, “Pitch shifts by the overlap of identical pulse trains with a delay and its relation to the binaural differences,” *Acoustical Science and Technology*, vol. 41, no. 1, pp. 433-434, 2020.

[40] H. Hu, C.H.H. Yang, X. Xia, et al, “Device-robust acoustic scene classification based on two-stage categorization and data augmentation,” in *Tech. Rep of DCASE2020 Challenge*.

[41] M. Sandler, A. Howard, M. Zhu, A. Zhmoginov, and L.C. Chen, “MobileNetV2: inverted residuals and linear bottlenecks,” in *Proc. of IEEE CVPR*, 2018, pp. 4510-4520.

[42] K. He, X. Zhang, S. Ren, and J. Sun, “Deep residual learning for image recognition,” in *Proc. of IEEE CVPR*, pp. 770-778, 2016.

[43] S. Woo, J. Park, J.Y. Lee, I.S. Kweon, “CBAM: convolutional block attention module,” in *Proc. of ECCV*, 2018, pp. 3-19.

[44] http://dcase.community/challenge2021/task-acoustic-scene-classification.